Annals of Nuclear Energy 112 (2018) 84–93

Contents lists available at ScienceDirect

Annals of Nuclear Energy

journal homepage: www.elsevier.com/locate/anucene

Progress in modeling in-containment source term with ASTEC-Na

L.E. Herranz [a,*], L. Lebel [b], F. Mascari [c], C. Spengler [d]

[a] CIEMAT Nuclear Safety Unit, Nuclear Fission Division, Avda. Complutense, 40, 28040 Madrid, Spain
[b] Institut de Radioprotection et de Sûreté Nucléaire (IRSN), St Paul lez Durance, France
[c] Italian National Agency for New Technologies, Energy and Sustainable Economic Development (ENEA) Via Martiri di Monte Sole, 4, Bologna, Italy
[d] Gesellschaft für Anlagen- und Reaktorsicherheit (GRS) gGmbH Schwertnergasse 1, 50667 Köln, Germany

ARTICLE INFO

Article history:
Received 15 April 2017
Received in revised form 10 September 2017
Accepted 18 September 2017
Available online 4 October 2017

Keywords:
In-containment source term
CPA* module
Na-pool fires
Aerosol chemical ageing

ABSTRACT

The ASTEC-Na code is being developed to simulate any sort of postulated accidents in Na-cooled fast reactors, particularly severe accidents. A significant progress has been made in the development of source term models, their implementation in the code and the specific validation of the specific code module, hereafter named CPA*, under the auspices of the JASMIN project.

In this paper the fundamentals of models for Na pool fire thermal-hydraulics and particle generation and chemical ageing of airborne particulates are described. Based mostly on data gathered from the open literature, CPA* performance under conditions anticipated during Na pool fires has been assessed against AB1, AB2, F2 and EMIS10 experiments. Thermal-hydraulic estimates have shown acceptable generic trends with noticeable quantitative deviations, despite the highly parametrized models used. A similar statement concerning aerosol behavior following measurements tendency is also applicable. As for chemical ageing, the comparisons set indicate that further work is still necessary. Therefore, even though some significant progress has been achieved, it is unquestionable that further work needs to be done in the three areas addressed. Finally, it should be highlighted that one of the main outcomes of this work is the need of obtaining qualified data for models and codes validation, so that a thorough and sound model assessment and code validation can be conducted.

1. Introduction

The Gen. IV systems are being designed to enhance nuclear sustainability and versatility over those of Gen. II and Gen. III reactors. Nevertheless, among all Gen. IV system features the one that is being paid more attention to is safety, which is pursued to reach the highest safety standards and the best safety demonstration robustness ever applied to Nuclear Power Plants (NPPs). By considering accidents with significant fuel damage (i.e., severe accidents) in the system design phase, explicit measures are taken so that they can be inherently avoided or prevented and/or mitigated by passive design features or by ad-hoc engineering safeguards with elimination of the need for offsite emergency response (GIF, 2002).

Sodium-cooled Fast Reactor (SFR) technology is more mature than other Gen. IV designs since several SFR reactors have been operated in the world (i.e., BN-600, Phénix, PFR, Monju, etc.) and, as a result, the experience that has been gained currently amounts to more than 400 operational years. In fact, prototype reactors, like the BN-800 reactor in Russia, have recently come online and a conceptual design has already being developed for the French ASTRID prototype reactor and it might start operation in the mid 2020s (CEA, 2015).

Sodium (Na) high thermal conductivity and low viscosity make it a good thermal-energy transport fluid with a broad temperature interval as a liquid (370–1156 K at atmospheric pressure). These characteristics turn Na into an excellent coolant, even at ambient conditions. Additionally, the low cross sections of neutron absorption and scattering make it a good choice as a coolant also from the standpoint of a fast-neutron economy. However, despite all these advantages, Na is very chemically reactive with oxygen and water, which entails a fire hazard risk in case of leaks.

Evaluating the effects of a sodium fire in containment would be a significant part of any safety evaluation of SFRs. A core disruption by supercriticality involves energetic destruction of fuel assemblies. The interaction between hot fuel and liquid sodium can lead to a vapor explosion which could create a breach in the primary system and contaminated liquid sodium at high temperature would be ejected into the containment. In contact with the oxygen the sodium burns and forms Na-oxide particles. The aerosol formed and its chemical transformations would be responsible to a great extent for the radiological and chemical impact of any

* Corresponding author.
E-mail address: luisen.herranz@ciemat.es (L.E. Herranz).

https://doi.org/10.1016/j.anucene.2017.09.037
0306-4549/

Abbreviations

c_t	Thermal accommodation coefficient	χ	Aerodynamic shape factor
F_{slip}	Particle slip coefficient	γ	Agglomeration shape factor
k_{gas}/k_p	Ratio of thermal conductivity of the gas over that for the particle	ε	Turbulence dissipation rate
		δ_{diff}	Diffusion boundary layer thickness
STICK	Particle sticking coefficient	ρ	Aerosol density

potential source term. In addition, if the leak is major, the heat released during the combustion is substantial, which has the potential to thermally damage the plant, cause an overpressure risk in containment, and be a source of airborne fission products as radionuclides dissolved in the sodium could be aerosolized. Therefore, a full-scope SFR safety analysis demands validated computation tools capable of capturing the main footprints of BDBAs (Beyond Design Basis Accidents) in containment, so that Source Term estimates are considered reliable.

A vast amount of research and development was done on SFR safety from the 1960s to the 1980s. In particular, several sodium fire studies (pool and spray fires) have been carried out since the 1970s, in facilities like PLUTON (Lhiaubet et al., 1990) and JUPITER (Malet et al., 1990) in France, CSTF in the USA (Hilliard et al., 1977, 1979; McCormack et al., 1978 and Souto et al., 1994), FAUNA in Germany (Cherdron and Jordan, 1980, 1983; Cherdron et al., 1985, 1990). More recent work was also performed in ATF in India (Subramanian and Baskaran, 2007; Subramanian et al., 2009; Baskaran et al., 2011). In all of them, the aim was to understand the sodium burning process and to study the sodium compound aerosols behaviour and their chemical composition.

The pioneering modeling work by Beiriger et al. (1973), who built a tool mainly focused on fire energetics (the SOFIRE code), was followed by others who made specific hypotheses and approximations. Since then most analytical developments have been associated to energetics and thermal-hydraulics (Murata et al., 1993), and just few of them addressed aerosol physics (Dunbar, 1985; Dunbar et al., 1984; Fermandjian, 1985). The MAEROS aerosol model (Gelbard 1982) represented a milestone describing the physical behaviour of a homogeneously mixed polydisperse aerosol system and even today it is the basis of the aerosol module in well-known severe accident and containment codes (MELCOR, ASTEC/CPA, COCOSYS).

Because the in-containment nuclear aerosol behavior is a very important part of chemical and radiological consequence assessments (and other factors, like for setting up suitable filtering systems) and because there was a lack of reliable predictive capabilities in this area, one of the main areas of the EU-JASMIN project (Girault et al., 2015) has been the development and validation of in-containment aerosol models. As a consequence, the ASTEC-Na code, which evolved from the LWR ASTEC code version to simulate SFR severe accidents, has been enhanced by including models for particle generation from Na pool fires and for chemical ageing of sodium oxide particles. The resulting containment module, hereafter called CPA*, has been compared to available data. The present paper summarizes the main features of these developments and an assessment of the current predictability of CPA* based on the comparisons set to data retrieved from the open literature.

2. New models

The most important addition to CPA* has been the pool fire combustion model, which as described below, is based on the SOFIRE-II model (Beiriger et al., 1973) that is present in CONTAIN-LMR (Murata et al., 1993). In addition, developments took place to better model the phenomena for how particles are generated in the flame, and how aerosols, once released into the air, react with water vapor and CO_2 to form sodium hydroxide and carbonate species. These latter two effects had been areas previously identified by Kissane et al. (2013) as phenomena for which there was a general lack of understanding, and are thought to play an important role in the potential contaminant transfer to the environment in case of an SFR accident, owing to the radio-chemical toxicity of possible sodium compounds, the vast amount of particles that might be formed in a Na pool fire and the Na interaction with key fission products, like iodine. It is worth mentioning that the model takes into account the gas composition variation over time during the accident sequence.

2.1. SOFIRE-II pool fire combustion model

The SOFIRE-II model assumes that the sodium burning rate is proportional to the oxygen concentration in the atmosphere, C_{O2}, and pool surface area, S_{pool}, and is controlled by the diffusion of oxygen to the sodium surface, as given by:

$$\dot{m}_{burn} = H_g \rho_g C_{O2} S_{pool} \quad (1)$$

where ρ_g is the gas density. The mass transfer coefficient for gas transport, H_g, is based on the heat transfer/mass transfer analogy assuming turbulent natural convection from a horizontal surface:

$$H_g = 0.14 \frac{D_{O2}}{d_{pool}} (Gr \cdot Sc)^{1/3} \quad (2)$$

where D_{O2} is the diffusivity of oxygen in air, d_{pool} is the diameter of the pool, Sc is the Schmidt number of the gas phase, and Gr is the Grasholf number evaluated based on the gas-pool temperature difference.

The SOFIRE-II model uses a simple, straightforward way to define different aspects of the pool combustion process. In reality, there is a complex inter-relationship between the sodium pool temperature, flame temperature, aerosol release rates, and (convective and radiative) heat transfer rates. In addition, sodium monoxide (Na_2O) and sodium peroxide (Na_2O_2) can both be formed in competing reactions. However, the SOFIRE-II model captures these effects using four simple user-defined parameters:

- f_1 defines the fraction of oxygen consumed for producing Na_2O (as opposed to Na_2O_2, which is the complement)
- f_2 defines the fraction of energy liberated from the combustion reaction that is transferred to heat up the pool (the complement goes on to heat the surrounding gas)
- f_3 defines fraction of Na_2O that is released to the atmosphere (the complement is retained in the pool)
- f_4 defines fraction of Na_2O_2 that is released to the atmosphere (the complement is retained in the pool)

In addition to other assumptions and simplifications that go into the SOFIRE-II model, the fact that f_1-f_4 parameters have to be set as constant for the duration of the fire simulations, is prob-

ably one of the most influencing ones. That being said, however, the model is simple and offers users sufficient flexibility to allow modeling of a pool fire in a manageable way for a lumped parameter code, like the CPA* module of ASTEC-Na.

2.2. Particle generation

This section presents the main features and bases of a Particle Generation (PG) model from sodium pool fires. It describes the vaporization of sodium and its subsequent combustion with the oxygen available that would result in the generation of supersaturated Na-oxide (Na_xO_y) vapors likely to nucleate and form suspended particles. The model assumes that reactions happen in a thin gaseous layer above the sodium pool and involve several steps, including: Na vaporization, O_2 transport by air natural circulation, Na-O_2 chemical reactions and vapor-to-particle conversion. A more thorough description was reported by García et al. (2016).

As described in García et al. (2016), the 3D fluid-dynamic analysis adopted the Reynolds Averaged Navier-Stokes (RANS) equations in the ANSYS Fluent code (ANSYS Inc., 2008). In the modeling, an SST k-ω turbulence model has been chosen to model the turbulent kinetic energy (k) and the specific dissipation rate (ω). The 3D model also encapsulates the chemical reactivity of Na and O_2 as an instantaneous process (Yamaguchi and Tajima, 2009):

$$Na + \frac{1}{4}O_2 \rightarrow \frac{1}{2}Na_2O + 9.08\ \mathrm{MJ/kg}Na \tag{3}$$

$$Na + \frac{1}{2}O_2 \rightarrow \frac{1}{2}Na_2O_2 + 10.48\ \mathrm{MJ/kg}Na \tag{4}$$

Once supersaturated Na_xO_y vapour has been formed in the gas phase after sodium oxidation, the system is in a non-equilibrium state and it will evolve towards equilibrium by generating primary particles (homogeneous nucleation) and by condensing sodium-oxide vapours onto the newly formed particles (heterogeneous nucleation). By applying the Classical Nucleation Theory (CNT), the nucleation rate results to be:

$$J_{CNT} = \left(\frac{2\sigma}{\pi m_1}\right)^{1/2} \cdot v_1 \cdot N_1^2 \cdot \exp\left[-\frac{16\pi}{3}\cdot\frac{v_1^2\sigma^3}{(kT)^3(\ln S)^2}\right] \tag{5}$$

A detailed discussion of the meaning and derivation of this equation has been recently provided by García et al. (2016).

Once a stable droplet is formed, its size will likely be less than the mean free path. For this condition, the removal of vapor by condensation is calculated as the net flow of molecules attached to the surface of a particle of a given size by collisional impact (kinetic theory):

$$F \approx \frac{\pi d_p^2}{(2\pi m_1 kT)^{1/2}}(p_{vap} - p_{sat}) \tag{6}$$

The rate of particle growth by condensation depends on the saturation ratio, particle size and particle size relative to the gas mean free path. The growth law expression is as follows (kinetic regime):

$$\frac{dd_p}{dt} = \frac{\pi d_p^2 v_1}{(2\pi m_1 kT)^{1/2}}(p_{vap} - p_{sat}) \tag{7}$$

The conditions for homogeneous nucleation are mainly determined by the saturation ratio and the temperature. The model assumes that once the first primary particle "burst" has occurred, heterogeneous nucleation dominates vapor depletion in the system.

This model has been partially validated by comparing the calculated burning rates of liquid sodium and aerosol concentration with the experimental results available (García et al., 2016).

These models, however, showed substantial temperature and concentration gradients which accurate estimates require a 3D approach that can capture the dynamics of oxygen convection to the flame region. However, this would be an impractical approach to take in safety analysis, and a formulation compatible with the ASTEC-Na lumped-parameter approach is necessary.

The 0-D adaptation of the PG model has been based on the preservation of the total number of generated particles in the active nucleation volume (i.e., the region in which saturation ratio is over 1.0):

$$N_{3D} = \sum_i \left(\int_{\Delta t} J_i^{CNT}(T_i, p_{v_i}) \cdot dt\right) \equiv N_{0D} = \left(\int_{\Delta t} J_i^{CNT}(\overline{T}, \overline{p}_v) \cdot dt\right) \cdot V_{PG} \tag{8}$$

In this equation, the number of generated particles (N_{3D}) in the active volume is given by the integration over time of the nucleation rate in all the cells (i) forming the active volume. As shown at the right side of the equation, the 0D approximation means to find out a characteristic nucleation rate of the volume dependent on averages of governing variables in the active region (i.e., temperature and partial pressure).

A correlation based on about 160 cases simulated with the PG model and defined according to the range of the major variables affecting the scenario (i.e., pool diameter, pool temperature and O_2 content), has been derived. Its generic equation can be written as:

$$N_{0D} = a \cdot \dot{m}_{Na}^b \cdot d_{pool}^c \cdot X_{O2}^d \tag{9}$$

As for primary particle size, the results from the 3D PG model in the 160 cases have indicated that most times the diameter would span in a narrow interval from $7.0{\cdot}10^{-10}$ m to $1.1{\cdot}10^{-9}$ m. Hence, it has been assumed a unique primary particle diameter of 10^{-3} μm.

2.3. Na-chemical transformation

Sodium monoxide (Na_2O) and sodium peroxide (Na_2O_2) are highly toxic and very corrosive. However, after they are released from the fire in the form of particles, these compounds can react with water vaport (H_2O) in the air to produce sodium hydroxide (NaOH), which is still toxic and corrosive:

$$Na_2O + H_2O \rightarrow 2NaOH + 152\ \mathrm{kJ \cdot mol^{-1}}$$

$$Na_2O_2 + H_2O \rightarrow 2NaOH + \frac{1}{2}O_2 + 53\ \mathrm{kJ \cdot mol^{-1}}$$

and further with carbon dioxide (CO_2) to produce carbonated sodium species, of which only the bicarbonate species is harmless.

$$2NaOH + CO_2 \rightarrow Na_2CO_3 + H_2O + 169\ \mathrm{kJ \cdot mol^{-1}}$$

$$Na_2CO_3 + H_2O + CO_2 \rightarrow 2NaHCO_3 + 85\ \mathrm{kJ \cdot mol^{-1}}$$

The chemical transformation model is based on a mechanism that was originally formulated by Cooper (1980), and further refined by Mathé (2014) through the determination of the undefined parameter (i.e. tortuosity…) in the diffusion coefficient formulation. This mechanism assumes that the reactions listed above between the oxides of sodium in the aerosol phase and water vapor or carbon dioxide, are controlled by mass transfer across the porous solid shell of the aerosol.

The equations that are implemented in the AERAGE model are expressed in terms of the molar reaction rate per aerosol particle (W) to the gas species concentration (c_{h2o} or c_{co2}) the diffusivity of the gas species in the porous shells (D^*_{h2o} or D^*_{co2}), and the respective diameters, d_3, d_2, d_1, d_0 of the outer (bicarbonate) layer, carbonate-bicarbonate interface, hydroxide-carbonate interface, and inner peroxide-hydroxide interface. There is also the additional Fuchs-Sutugin factor, f, which accounts for slip-correction factors in submicron aerosols. Here below such equations are displayed:

Sodium peroxide reaction:

$$W_1 = \begin{cases} \frac{2\pi c_{H_2O} D^*_{H_2O} d_0 d_3 f}{d_3 - d_0} & if\ c_{H_2O} > c_{CO_2} \\ \frac{2\pi c_{CO_2} D^*_{CO_2} d_0 d_3 f}{d_3 - d_0} & if\ c_{H_2O} < c_{CO_2} \end{cases}$$

Sodium hydroxide reaction:

$$W_2 = \frac{2\pi c_{CO_2} D^*_{CO_2} d_1 d_3 f}{d_3 - d_1}$$

Sodium carbonate reaction:

$$W_3 = \begin{cases} \frac{2\pi c_{H_2O} D^*_{H_2O} d_2 d_3 f}{d_3 - d_2} & if\ c_{H_2O} > c_{CO_2} \\ \frac{2\pi c_{CO_2} D^*_{CO_2} d_2 d_3 f}{d_3 - d_2} & if\ c_{H_2O} < c_{CO_2} \end{cases}$$

Note that, as the model is based on calculating the molar reaction rate of the limiting step, in case steam concentration is higher than CO_2 concentration one can reasonably think that the reaction will be limited by the CO_2 and then the D_{co2} should be used in the formula rather than D_{H2O} (and vice versa). Based on experiments that were performed more recently investigating the sodium oxide carbonation, Mathé (2014) proposed that the value for the CO2 diffusion coefficients should be on the order of $5{\cdot}10^{-9}$ $m^2{\cdot}s^{-1}$. A similar coefficient was assumed for steam diffusion.

The implementation of this model in ASTEC-Na requires that the users provide the value of the diffusion coefficient as an input, with a recommended value of $5{\cdot}10^{-9}$ $m^2{\cdot}s^{-1}$. The main simplification compared to the original model built by Mathé is to neglect the history of the aerosol compositions as a function of injection time by means of multiple aerosol generations. Chemical reactions are performed on the bulk population of aerosols, and separately on different size classes. The internal diameters d_0 d_1, d_2, d_3 required for the calculation of mass transfer rates, evolve as a consequence of the chemical transformations that particles undergo. Finally, the density of the mixture aerosol is assumed constant all through the chemical transformation (this assumption, though, does not significantly impact the aerosol physics).

3. Validation of ASTEC-Na/CPA*

In this section, three different calculations will be reported. Two of them used the CPA* module (the ASTEC-Na module for in-containment source term analysis), whereas one shows the CPA results (i.e., the LWR version of CPA non-updated with new Na models).

3.1. Test matrix

The ABCOVE experiments were conducted in the Containment System Test Facility (CSTF) vessel at the HEDL (Hanford Engineering Development Laboratory, USA). The containment is a cylindrical steel vessel (7.6 m diameter, 20.3 high) of about 852 m^3. In test AB1, 410 kg of sodium at 600 °C was spilled into a burn pan of 4.4 m^2 through an electrically heated delivery line. The burn pan had a hinged lid which was in the vertical position during the spill. The sodium flow lasted 80 s and the splashing was minimized by baffles in the pan. At 60 min after the initiation of the spill, the lid was closed and the sodium pool fire extinguished. The AB2 test was performed with essentially the same initial conditions, but with the addition of an injection of steam, at a rate of 0.02 kg/s, near the center of the containment vessel, 16 min after the start of the fire. The steam injection was meant to simulate the release of water vapor from heated concrete at a rate equivalent to the release of water vapor from ~10–30 m^2 of hot concrete. In this test, 472 kg of sodium at 600 °C were delivered and the pool fire burn duration was 60 min. A more thorough description of experimental aspects may be found in Hilliard et al. (1977, 1979), McCormack et al. (1978) and Souto et al. (1994).

The FAUNA facility consists of a fire room, a measuring room, and an aerosol measuring loop. A cylindrical steel vessel of 6 m in diameter and 6 m high with domed ends (volume 220 m^3) served as the fire room. In the F2 test, a sodium pool fire was produced inside the FAUNA containment in a circular burning pan of 1.6 m diameter (2 m^2) after adding 250 kg of sodium at 500 °C. During the experiment, the oxygen content was kept constant through 3 injections of approximately 1% of the vessel molar content with different durations. The pool fire lasted for 210 min. More thorough information may be found in Cherdron and Jordan (1980, 1983) and Cherdron et al. (1985, 1990).

The series of smaller scale EMIS experiments were performed in a 4.4 m^3 cylindrical steel vessel by IPSN (Institut de Protection et de Sûreté Nucléaire). The combustion pan was 0.125 m^2. The EMIS10b test was a sodium pool fire (0.40 m diameter) produced by the released of 9.4 kg of sodium at 271 °C. The pool fire duration is until its total depletion (~6000 s). During the test, the oxygen content (20%) was maintained approximately constant by the injection of oxygen. More information can be found in Casselman and Malet (1985) and Dunbar (1992).

Given the different scale of the facilities chosen for the validation it is foreseen that sodium burning rate is also different, as can be seen in Section 3.3. Probably this is the result of changes in the experimental boundary conditions, particularly the characteristic time of air natural convection loops and the effective Na surface exposed might be different.

A more detailed description of the experiments and experimental facilities are available in Herranz et al. (2017), in addition to the original experimental reports listed above. As an example, a diagram of the CSTF facility is shown in Fig. 1. The FAUNA and EMIS experiments were conducted in nearly identical facilities, just at different scales.

3.2. Scenarios modeling

All the experimental vessels were modelled as a single cell in which all the structures described in the experimental reports were accounted for. The sodium pool surface was modeled as a hot structure facing the gas atmosphere in all the simulations. Since the ASTEC/CPA calculations did not explicitly have a pool fire

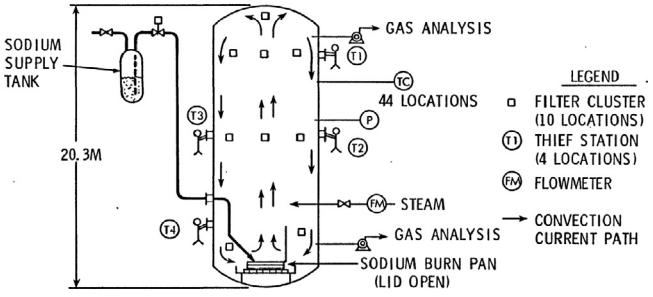

Fig. 1. CSTF vessel arrangement (Hilliard et al., 1977).

model, the combustion process was modelled with heat sources in the gas and pool surface, and aerosol injections into the gas.

A number of thermal-hydraulic hypotheses and approximations are made, and it is worth summarizing them here:

- The ASTEC-Na/CPA* calculation assumed an f_1 value of 0.33 for all the tests, meaning that there was about a 2:1 ratio between sodium peroxide and sodium monoxide production (see Table 1), which best matched experimental observations. In ASTEC/CPA, oxygen consumption was not modelled, and particle generation from the fire was modelled as an individual aerosol source with a constant mass flow rate during the Na burning.
- The ASTEC-Na/CPA* calculation assumed an f_2 value of 0.5 for all of the tests except for the EMIS 10b test, which was set to 0.1, meaning that 50% and 90%, respectively, of the combustion energy was transferred directly to the gas phase. The ASTEC/CPA calculations assumed that ***46%*** of the combustion energy would be released into the air and ***54%*** of the combustion energy would be released into the pool (corresponding to an f_2 value of ***0.54***, set to match the peak containment atmosphere temperature).
- The emissivity of the sodium pool was set to 0.25 in both the ASTEC-Na/CPA* and ASTEC/CPA calculations to allow thermal radiation. This value is recommended by Yamaguchi and Tajima (2006).

As for aerosol modeling, some additional hypotheses have been made:

- The aerosolization rates of each species is determined through the f_3 (fraction of Na_2O released to the atmosphere) and f_4 (fraction of Na_2O_2 released to the atmosphere) parameters in the input deck (Table 2). The settings have been defined to get the best fit to data.

Table 1
f_1 and f_2 values (for all the test).

	ASTEC-Na/CPA*	ASTEC/CPA
AB1 & AB2		
f_1	0.33	–
f_2	0.5	0.54
F2 Test		
f_1	0.33	–
f_2	0.5	0.54
EMIS10b Test		
f_1	0.33	–
f_2	0.10[a]	0.54

[a] This value corresponds with the best match for the experimental values.

Table 2
f_3 and f_4 values.

	ASTEC-Na/CPA*
AB1/AB2 tests	
f_3	0.25
f_4	0.25
F2 test	
f_3	0.00
f_4	0.10
EMIS10b test	
f_3	0.35
f_4	0.35

Table 3
Aerosol coefficients and density (for all the tests).

	CPA*/CPA
χ	1.00
γ	1.00
F_{slip}	1.37
STICK	1.00
ε	0.02
k_{gas}/k_p	0.03
c_t	1.00
δ_{diff}	$-/1.00{\cdot}10^{-4}$ m
ρ	2800/2420 kg/m^3

Unlike ASTEC-Na/CPA** above, ASTEC/CPA needs to define an aerosol injection rate. An aerosol source is therefore imposed as a constant mass flow rate lasting during the Na burning. According to the test specifications, the flow rates imposed are $1.10{\cdot}10^{-2}$ kg/s (AB1), $1.07{\cdot}10^{-2}$ kg/s (AB2), $1.28{\cdot}10^{-3}$ kg/s (F2), $2.60{\cdot}10^{-2}$ kg/s (F3) and $2.1{\cdot}10^{-4}$ kg/s (EMIS10b).

- As for particle size, as stated above primary particles formed are assumed to be 10^{-9} m diameter with a Geometric Standard Deviation (GSD) of 2.0. This is informed by the particle generation model. The ASTEC/CPA entered clusters of 10^{-6} m diameter with a GSD of 2.0 (AB1 and AB2) and 1.4 (F2 and EMIS10b), according to the experimental information available (Hilliard et al., 1979; Cherdron and Jordan, 1980).
- Additionally, some other particle features are often set in the input deck (i.e., shape factors, conductivity, sticking efficiency, etc.). Table 3 gathers the different code assumptions. Generally speaking, the default values in each code have been used according to previous research (Fermandjian et al., 1980). Some variability exists, though, in density: whereas ASTEC-Na/CPA* estimated it as a function of Na_2O and Na_2O_2 distribution, as described by f_1; ASTEC/CPA took the estimated aerosol material density for the AB1 test made by Hilliard et al. (1979).
- Finally, the Cooper diffusion coefficient in the ASTEC-Na/CPA* calculations has been set to $5{\cdot}10^{-9}$ m^2 s^{-1}. Aerosol reactions with water vapor and CO_2 were note modelled with ASTEC/CPA.

3.3. Main results

The comparisons below have been set mostly against data found in the open literature. In order to suitably focus the results analysis, some previous discussion on the data used for comparison is indispensable. Two key aspects of the data are: the local/average nature and the source from which the data have been withdrawn. The local/average temperature is directly related to their significance as a footprint of the whole scenario (as local values of some variables could not give a meaningful hint of the governing phenomena) and to the credit that data-estimates comparisons should be given in terms of validation (i.e., comparison of a local gas temperature with the gas temperature prediction of a single node calculation for a vessel of hundreds of m^3 might be criticized, to say the least). The uncertainty associated to the data withdrawal process can be crucial: a numerical value taken from a text or table in a scientific/technical report can be assumed to be "as given", whereas if data are taken from figures the withdrawal accuracy will be dependent on the quality of the plot, the type (linear vs. log), the tool used to pick the data points, etc.

Overall, consideration of the aspects discussed above has resulted in experimental error bars that can be said to be reasonable (roughly ±20%) in temperatures and notably larger (>50%) in concentrations, particularly at the early times of Na burning.

3.3.1. Thermal-hydraulics

Figs. 2 through 5 show comparisons of atmosphere temperature between data and estimates for tests AB1, AB2, F2 and EMIS10b, respectively. In general, AB1, AB2, and F2 follow the same experimental trends. Gas temperature may be described in two main phases: heat-up and cool-down. The heat-up phase is, in turn, split into 4 stages: a first period (about 60 s) in which a sharp increase of temperature occurs; a second one along which temperature hardly changes for about 500 s; a third one in which temperature increase proceeds gently for some 2000 s; and a last period until the fire quenching, where heat-up slightly slows down. The cooling down shows two steps: a fast one due to chemical reactions brought to a halt and the isolation of the hot sodium by covering the burn pan, and a longer and more progressive one, as heat is steady lost to the vessel walls by natural convection.

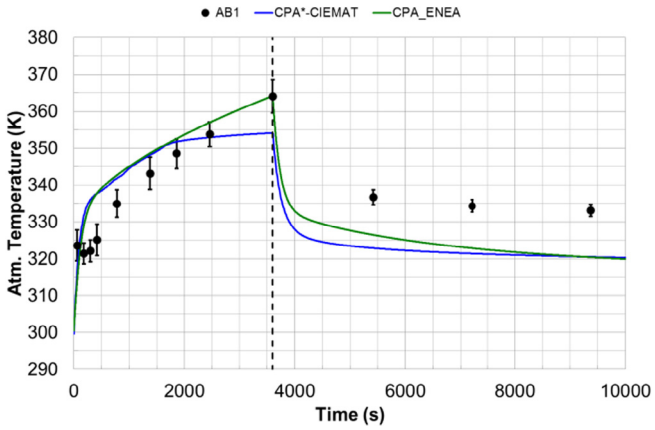

Fig. 2. AB1 test atmosphere temperature.

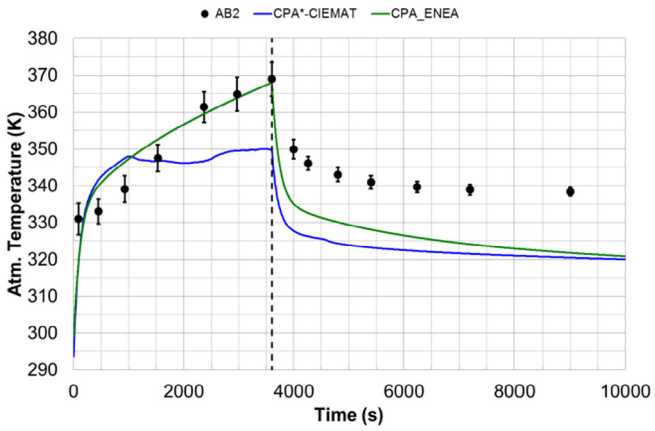

Fig. 3. AB2 test atmosphere temperature.

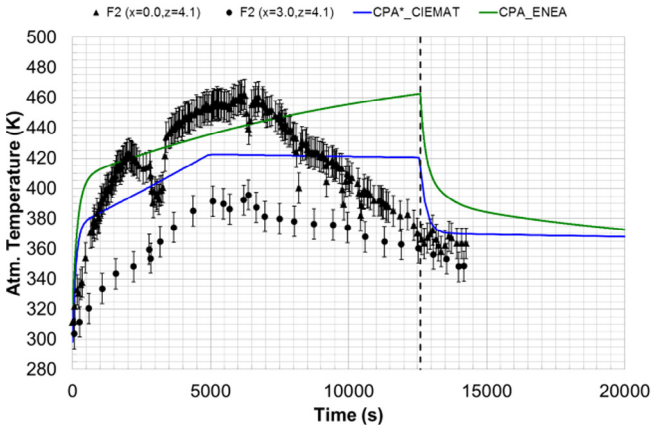

Fig. 4. F2 test atmosphere temperature.

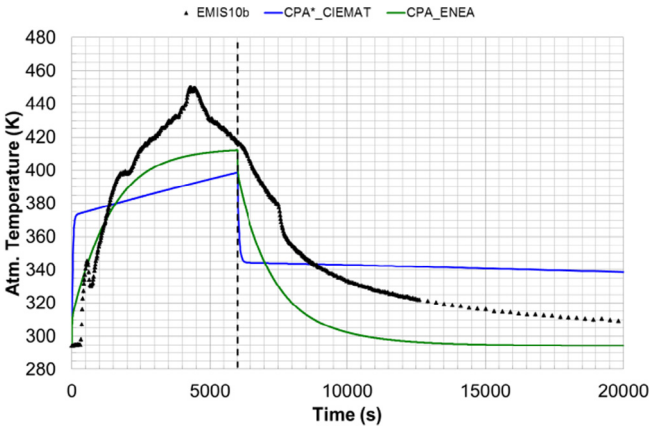

Fig. 5. EMIS10b test atmosphere temperature.

Consistently with major experimental observations, calculations also show the two main experimental phases. However, differences show up when focusing in each of them. On one side, only two periods are predicted in the heating phase and, regardless if they match the maximum temperature at the end of the phase, all in all measured heating rates are poorly captured (note that inputs to the ASTEC/CPA calculation was tuned to ensure that results fit the peak temperature data). This is not surprising since Na-injection effects (i.e., Na exposure to O_2 during its pouring into the pan) have not been considered in the scenario modelling and the f_1 and f_2 settings have been done on arbitrary basis and they would need some confirmatory studies. These values are constant throughout the fire, whereas the burning and heat release rates were likely variable, at least to a certain extent, throughout the experiment. On the other hand, cooling rate due to fire quenching is largely overpredicted at the beginning of the cooling phase, which might indicate a too high energy source during the fire period (0–3600 s); in the longer cooling period there are also deviations but they are not as noticeable as those discussed above.

Despite this generic behaviour, in the case of F2, thermocouples located at different heights in the vessel (x = 0.0 m and x = 3.0 m) indicated, as shown in Fig. 4, that atmosphere was not well mixed during Na burning. In addition, temperature at x = 0.0 m is highly sensitive to O_2 concentration, so that whenever O_2 concentration decreases temperature falls down quite noticeably. Finally, even though the end of fire is set to be at 12600 s in the test protocol, according to temperature records, fire started extinguishing progressively since around 6000 s (also observed in EMIS10b). As O_2 concentration is far from being zero in the vessel at 6000 s, the temperature trend might mean that it takes some time for O_2 at other locations than the burning pan vicinity to reach it or, in other words, that Na burning is much faster than convection loops set in the vessel as a consequence of Na burning. This experimental footprint is not captured by predictions, in which fire end were set to happen at 12600 s, and the entire vessel was modelled as a single cell.

From the above discussions one may withdraw some takeaways from the modeling perspective:

- Energy source into the gas atmosphere during Na pool burning should be further investigated, so that models are based on a sort of mechanistic understanding instead of on empirical and sometimes arbitrary settings.

- The single-node approach seems to be capable of following data trends under soft transients; however, under fast transient conditions driving to atmosphere non-uniformity for a while, it should be expected to undergo significant deviations.

As noted in the above figures, experimental error bars are reasonable and, anyway, they are not responsible for the deviations of estimates and data.

3.3.2. Aerosol behavior

The three main metrics used in the CPA* benchmarking are: the suspended mass concentration, the aerodynamic mass median diameter (AMMD), and the deposition of material on different surfaces at the end of the tests.

Fig. 6 shows the evolution of the aerosol concentration in AB1 test. It is worth noting the large uncertainties associated with the experimental data before 1000 s. During the burning phase (0–3600 s), a quasi-steady state between 0.02 and 0.03 kg/m^3 was measured, so that there was a balance between particle generation and aerosol deposition; afterwards, once the Na fire is over, concentration decayed exponentially as theoretically anticipated by the general dynamics equation for aerosols (Gelbard, 1979). ASTEC-Na/CPA* can be said to fall within experimental uncertainties during the quasi-steady state period, but neither follows the observed steady trend before the sodium pool fire ending. Besides, the experimental depletion rate during the first 1000 s of the depletion phase is about twice higher than the predictions, likely associated to the particle size underprediction since the dominant particle depletion process (i.e., sedimentation) is proportional to diameter squared.

Fig. 7 displays the AMMD evolution. The data experienced a jump from about 6 μm to approximately 8 μm between 4000 and 5000 s. This change is the result of the end of injection of small particles from the fire, so that naturally the size distribution shifted to bigger sizes. The previous maximum observed before the end of burning is likely due to the significance acquired by deposition mechanisms over time, particularly sedimentation, that removed larger particles from the gas atmosphere. Right after Na fire quenching, again the progressive decrease of the particle size is a consequence of preferential deposition of large particles by sedimentation. ASTEC-Na/CPA* calculations reasonably follow measurements. Figs. 8 and 9 concerning AB2 test provide similar insights into the modelling. It is worth highlighting that sodium aerosol release rate is so high that the initial nano-particles agglomerate so fast that micro-particles are formed in quite a short time, so that at 100 s particles' AMMD is already around 1 μm.

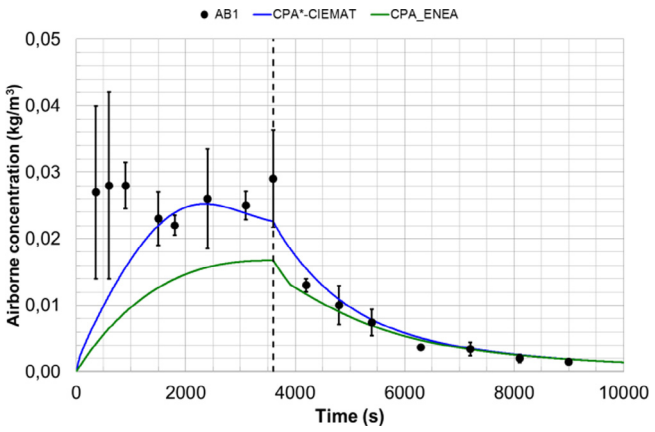

Fig. 6. AB1 airborne aerosol evolution.

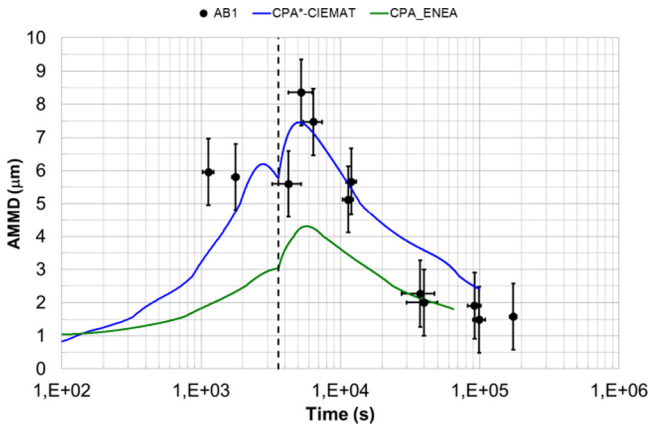

Fig. 7. AB1 AMMD evolution.

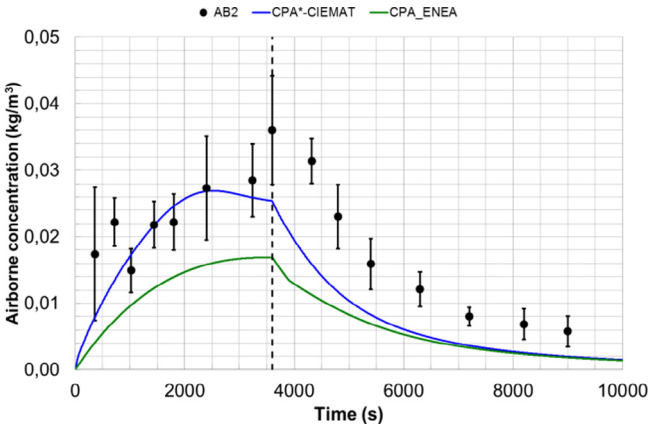

Fig. 8. AB2 airborne aerosol evolution.

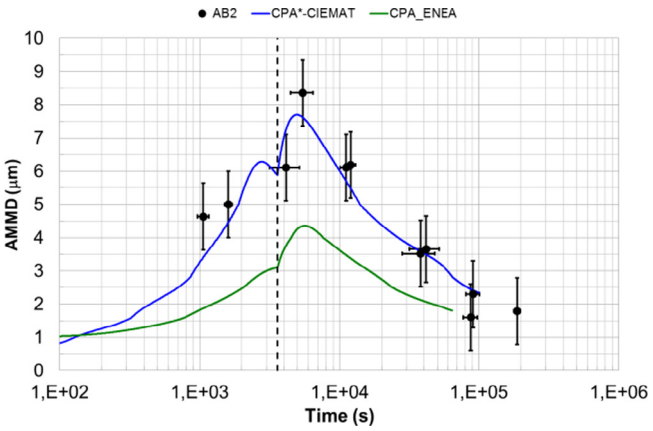

Fig. 9. AB2 AMMD evolution.

Figs. 10 and 11 show the final mass distribution in tests AB1 and AB2. Even though ASTEC-Na/CPA* qualitatively captured the general trend better than ASTEC/CPA (i.e., most of particles deposit by sedimentation on the vessel floor), significant differences can be noted with respect to data: mass depleted onto vessel vertical walls via thermophoresis has been largely overestimated.

Except for AB1 and AB2, which share most of the observations made regarding data-CPA* estimates comparison, in the rest of the other tests such comparisons are not conclusive at all. The lack of data during the first 1000 s, the broad uncertainty affecting data

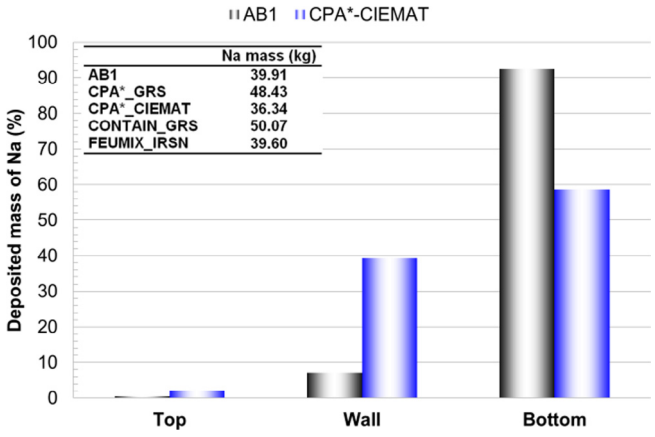

Fig. 10. AB1 final aerosol mass distribution.

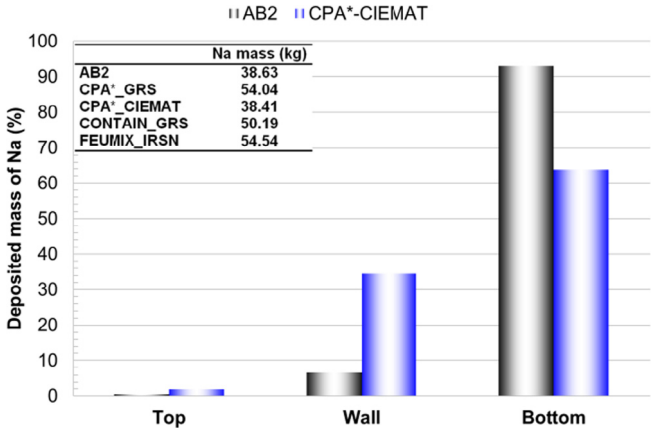

Fig. 11. AB2 final aerosol mass distribution.

and the local nature of some of the measurements taken, make any other comparison not meaningful in terms of CPA* validation.

3.3.3. Particle ageing

The evolution of the sodium peroxide, sodium hydroxide, and sodium bicarbonate mass fraction predictions are compared against experimental data in Fig. 12. Note that the model predictions for sodium carbonate are not shown; they are effectively at zero for the whole course of the calculation because the model predicts that sodium carbonate is consumed to produce sodium bicarbonate as fast as it is produced. Sodium monoxide was not modeled here since only the sodium peroxide form was observed in the AB1 and AB2 experiment aerosol measurements.

Although combustion product aerosols released from the sodium fire are initially emitted as sodium peroxide, the particle chemical ageing model predicts that these will nearly immediately (less than 1 s) be converted into sodium bicarbonate through the chain of hydroxide and carbonate reactions. The aerosols stay over 90% sodium bicarbonate in both the AB1 and AB2 tests until all of the carbon dioxide in the CSTF vessel atmosphere is consumed (after about 20–30 s). After this point, the mass fraction of sodium bicarbonate falls because, as there is no carbon dioxide available to react with new material as it is injected, the aerosols are only converted as far as sodium hydroxide. For reference, complete conversion of all of the CO_2 initially in the vessel (~15 mol) to sodium bicarbonate would require ~7.5 mol of sodium peroxide (~0.59 kg), while complete conversion of all of the H_2O initially in the vessel (~500 mol) would require ~500 mol of sodium peroxide (~39 kg).

Unfortunately, there is no data available to confirm this fast spike and drop in the sodium bicarbonate concentration, since the first aerosol measurements were taken 16 minutes (960 s) after the start of the test. That being said, there was no evidence in either of the experiments that sodium bicarbonate was observed at all, as opposed to sodium carbonate, which was observed in trace amounts. The experiments by Anantha-Narayanan et al. (2015) did have the capability to discriminate between sodium carbonate and bicarbonate forms, but only ever observed the bicarbonate forms after 30 to 60 min from the initial injection of aerosols. On the other hand, Clough and Garland (1971), who conducted a review of the carbonate-bicarbonate equilibria, stated that sodium bicarbonate would only form in cases when the relative humidity exceeded 99%. The thermal decomposition of sodium bicarbonate at temperatures above 100 °C is well studied in the literature (Barrall and Rogers, 1966; Hu et al., 1986; Heda et al., 1995), and has been reported to occur as low at 50 °C under dry enough conditions. It is unlikely, therefore, that sodium bicarbonate could form in any significant quantity, but rather carbon dioxide would likely be absorbed by the aerosols to form sodium carbonate only. The mechanics of that reaction are not accurately represented by the models contained in the present model.

After the carbon dioxide in the atmosphere is consumed, sodium hydroxide quickly becomes the dominant aerosol species until all of the water vapor is also consumed. In the case of test AB2, the supplementary injection of steam into the CSTF vessel ensures that the injected sodium peroxide is completely converted to sodium hydroxide. This is accurately predicted by the AERAGE model. However, for test AB1, the experiments showed that sus-

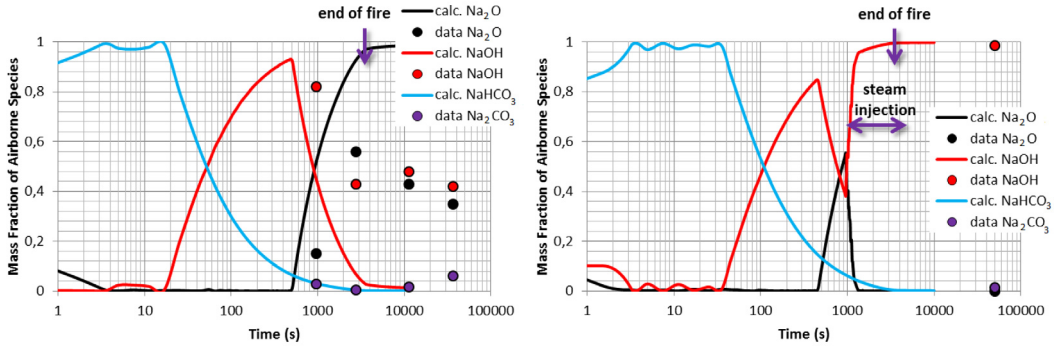

(a) Test AB1 (b) Test AB2

Fig. 12. Comparison between the ASTEC-Na/CPA predictions of the aerosol composition using the AERAGE model and experimental values reported by Hilliard et al. (1979).

pended aerosols would contain about equal amounts of sodium peroxide and sodium hydroxide in the long-term. The AERAGE model, by contrast, predicted that water vapor in the CSTF vessel would be quickly and completely consumed from the reaction with sodium peroxide, and that the sodium hydroxide concentration should drop to near zero after about 3000 s. Model predictions were not far from the first observations made at 960 s after the start of the fire, but were in poor agreement with the observation made 2760 s after the fire and after, as well as with the final composition on the walls. This discrepancy implies that this model does not completely capture all of the dynamics of the sodium peroxide/water vapor reaction either.

The problem, however, is that the model predicts that the reactions should occur more quickly than they actually do, and likely comes with the value for the crust diffusion that is recommended by Mathé (2014). This recommendation was based on an extrapolation of the results of bench-scale experiments on large grains of sodium peroxide, and so it is possible that the crust diffusion coefficients that were measured in that study are not characteristic of what would be experienced by sodium aerosols released from a pool fire. Likewise, the crust diffusion model does not take into account bulk mixing effects, which would be important when considering chemical reactions occurring over large volumes.

4. Overall discussion

As described in previous sections, a step forward has been achieved in modeling in-containment source term during potential severe accidents in Na-cooled reactors. In particular, models for particle generation during pool fires and the subsequent chemical reactions of airborne particles with steam and carbon monoxide have been implemented in CPA* and the code module performance tested against some of the more sound available data in the open literature. From all this work some highlights are given in the next paragraphs.

ASTEC-Na does have models for containment thermal-hydraulics, aerosol generation from Na pool fires and chemical ageing while airborne in the atmosphere in presence of steam and carbon dioxide; however, the current ASTEC-Na capability to model in-containment source term is still under development. There are major phenomena potentially affecting in-containment source term that are still missing in ASTEC-Na, like particle generation from Na spray fires, fission product entrainment from Na-concrete interaction, thermal and chemical behavior of fission products in Na-containing aerosols. Additionally, the key phenomena implemented for in-containment source term are described by heavily parametrized models (i.e., chemical energy distribution and Na oxides partition between pool and atmosphere). In other words, a deep understanding of those phenomena that would allow a mechanistic modeling is missing.

The comparisons set to data have shown that the anticipated thermal evolution in SFR containment during a Na-pool fire might be captured whenever models parameters are adequately set and containment is meshed properly (i.e., the single-node approach might not be suitable under fast transient conditions resulting in non-uniform atmospheres for a while). In particular, the most sensitive parameters are those involved in the chemical energy distribution between Na pool, containment atmosphere and surrounding structures. Similarly, aerosol models show a promising response in terms of order of magnitude of airborne concentration, dominant depletion mechanism (i.e., sedimentation) and particle size variation. Quantitative deviations from data, though, have been observed both in the airborne concentration of aerosols and in their chemical composition. Although comparisons are inconclusive yet, it seems highly likely that the models developed need review, extension and further assessment. This is the case, for example, of particle agglomeration over the pool at high concentrations, the presence of Na as a potential condensing vapor in the containment module of the ASTEC-Na code or the Na_2O reactions.

The current experimental database does not support a sound and reliable definition of default values for the parameters embedded in the mentioned models. The comparisons to data set are far from a thorough validation. A number of reasons underpins this statement: the number of such comparisons is a way too reduced due to scarcity of open data and project resources constraints; often variables recorded are insufficient to qualify any of the models developed (most data come from integral tests and separate effect tests data are either lacking or difficult to scale up); and, in addition, measurements are often affected by large uncertainties that prevent even the general trend from being seen. Two specific examples are: the large experimental uncertainties existing in aerosol concentration during the Na-pool fire period, which make it difficult to draw any specific insights regarding models of particle generation and/or aerosol mechanisms in codes; and the lack and/or low confidence of the available experimental data on H_2O_v and CO_2 consumption and or aerosol speciation, which hinders a proper AERAGE model validation. This being said, the comparisons set have given meaningful information.

Therefore, in-containment source term modeling in SFRs during severe accident needs to be extended with some still missing models. Furthermore, both the particle generation and the ageing models (along with their implementation in the ASTEC-Na code) need a thorough review to firmly state their current capabilities. Such further development will require both analytical and experimental work in future. The experimental activities to undertake should be carefully designed to ensure key data aspects like representativity, accuracy and scalability. In other words, there is an outstanding need to build a robust and extensive database that can be used both to support individual model development and to validate more "integral" tools, like ASTEC-Na CPA.

Acknowledgments

The authors wish to thank the funding received from the 7th Framework Programme of the European Commission via the JASMIN project (contract number 295803). Parts of this work are co-financed by the German Federal Ministry for Economic Affairs and Energy (BMWi). In addition, our appreciation to Nathalie Girault (IRSN) for the reviews done of this work and to Monica García (CIEMAT) for her involvement in part of the work here presented.

References

Anantha Narayanan, R., Subramanian, V., Sahoo, P., Misra, J., Kumar, A., Baskaran, R., Venkatraman, B., Murali, N., 2015. Experimental investigations on carbonation of sodium aerosol generated from sodium fire in the context of fast reactor safety. Ann. Nucl. Energy 80, 188–194.

ANSYS Inc. 2008. FLUENT Computational Fluid Dynamics Software, FLUENT User's Guide.

Barrall, E.M., Rogers, L.B., 1966. Differential thermal analysis of the decomposition of sodium bicarbonate and its simple double salts. J. Inorg. Nucl. Chem. 28, 41–51.

Baskaran, R., Subramanian, V., Venkatram, B., Chellapandi, P., 2011. Sodium aerosol studies for fast reactor safety. Energy Proc. 7, 660–665.

P. Beiriger et al., 1973. SOFIRE-II User Report. AIAEC-13055. Atomics International Division, Canoga Park, CA, USA.

Casselman, C., Malet, J.C., 1985. Experimental study of sodium pool fire aerosol behavior. Comparison with calculation code. In: Proceedings of CSNI Specialists Meeting on Nuclear Aerosols in Reactor Safety, Kfk3800, CSNI-95.

CEA, 2015. The ASTRID Project: advanced sodium technological reactor for industrial demonstration. In: 48th Meeting of the Technical Working Group on Fast Reactors, 25–29 May 2015, IAEA, https://www.iaea.org/NuclearPower/Meetings/2015/2015-05-25-05-29-NPTDS.html.

Cherdron, W., Jordan, S., 1980. Determination of sodium fire aerosol process coefficients from FAUNA-experiments. In: Proceedings of the CSNI Specialists

Meeting on Nuclear Aerosols in Reactor Safety. NUREG/CR-1724, ORNL/NUREG/TM-404, CSNI-45.
Cherdron, W., Jordan, S., 1983. Die Natrium-Brandversuche in der FAUNA-Anlage auf Brandflächen bis 12 m2. KfK 3041.
Cherdron, W., Bunz, H., Jordan, S., 1985. Properties of sodium fire aerosols and recalculation of their behaviour in closed containments. In: Proceedings of the CSNI Specialists Meeting on Nuclear Aerosols in Reactor Safety. Kfk3800, CSNI-95.
Cherdron, W., Jordan, H., Lindner, W., 1990. Die Natriumbrand-Untersuchungen in der FAUNA. Teil 1: Poolbrände und Aerosolverhalten. KfK 4358.
Clough, W.S., Garland, J.A., 1971. The behaviour in the atmosphere of the aerosol from a sodium fire. J. Nucl. Energy 25, 425–435.
Cooper, D.W., 1980. Prediction of the rates of chemical transformation of sodium fire aerosols. US Nuclear Regulatory Commission report NUREG/CR-1724.
Dunbar, I.H., 1985. Aerosol behaviour codes, development, intercomparison and application. In: Presented at the CSNI Specialist Meeting on Nuclear Aerosols in Reactor Safety, CSNI-95, Karlsruhe, pp. 471–485.
Dunbar, I.H., 1992. Sodium fire aerosol behaviour: a review of studies carried out under the auspices of the CEC. Published by the Commission of the European Communities, EUR 14023 EN, ISBN 92-826-3992-4.
Dunbar, I.H., Fermandjian, J., Bunz, H., L'homme, A., Lhiaubet, G., Himeno, Y., Kirby, C.R., Mitsutsuka, N., 1984. Comparison of sodium aerosol codes (CEC report No. EUR–9172). Commission of the European Communities.
Fermandjian, J., Malet, J.C., Casselman, C., Duverger de Cuy**, G., Boulaud*, D., Madelaine*, G., 1980. Interpretation of the behavior of aerosols generated by a sodium pool fire. In: Proceedings of the CSNI Specialists CSNI-45, pp. 480–490.
Fermandjian, J., 1985. Aerosol behaviour codes, development, intercomparison and application. In: Presented at the CSNI Specialist Meeting on Nuclear Aerosols in Reactor Safety, CSNI-95, Karlsruhe, pp. 486–497.
García, M., Herranz, L.E., Kissane, M., 2016. Theoretical assessment of particle generation from sodium pool fires. Nucl. Eng. Des. 310, 470–483.
Gelbard, F., 1979. The General Dynamic Equation for Aerosols. Thesis of the California Institute of Technology, Pasadena, California.
Gelbard F., 1982. MAEROS User Manual, NUREG/CR-1391. Sandia National Laboratories, Albuquerque, USA.
GIF, 2002. A Technology Roadmap for Generation IV Nuclear Energy Systems. GIF-002-00, U.S. DOE Nuclear Energy Research Advisory Committee and the Generation IV International Forum.
Girault, N., Cloarec, L., Herranz, L.E., Bandini, G., Perez-Martin, S., Ammirabile, L., 2015. On-going activities in the European JASMIN project for the development and validation of ASTEC-Na SFR safety simulation code. In: ICAPP2015. Presented at the International Congress on Advances in Nuclear Power Plants (ICAPP 2015), Nice (France), pp. 482–494.
Heda, P.K., Dollimore, D., Alexander, K.S., Chen, D., Law, E., Bicknell, P., 1995. A method of assessing solid state reactivity illustrated by thermal decomposition experiments on sodium bicarbonate. Thermochim. Acta. 255, 255–272.
Herranz, L.E., Garcia, M., Lebel, L., Mascari, F., Spengler, C., 2017. In-containment source term predictability of ASTEC-Na: major insights from data-predictions benchmarking. In: Nucl. Eng. Des., 0029-5493 320, 269–281. https://doi.org/10.1016/j.nucengdes.2017.06.010.
Hilliard, R.K., McCormack, J.D., Hassberger, J.A., Muhlestein, L.D., 1977. Preliminary results of CSTF aerosol behavior test, AB-1. HELD-SA-1381.
Hilliard, H.K., McCormack, J.D., J.A., Postma, A.K., 1979. Aerosol behavior during sodium pool fires in a large vessel – CSTF tests AB1 and AB2. Hanford Engineering Development Laboratory report HEDL-TME 79–28.
Hu, W., Smith, J.M., Dogu, T., Dogu, G., 1986. Kinetics of sodium bicarbonate decomposition. AIChE J. 32 (9), 1483–1490.
Kissane M.P., Garcia M., Herranz L.E., 2013. Major remaining uncertainties associated with source-term evaluation for SFR severe accidents. In: Proceedings FR13, IAEA, 4–7 March 2013, Paris, France.
Lhiaubet, G., Bunz, H., Kissane, M.P., Seino H., Miyake, O., Himeno, Y., Casselman, C. Such, J.M., Rzekiecki, R., 1990. Comparison of aerosol behaviour codes with experimental results from a sodium fire in a containment. In: International Fast Reactor Safety Meeting, Snowbird, Utah, 12–16 August 1990.
Malet, J.C., Sophy, Y., Rzekiecki, R., Cucinotta, A., Mosse, D., 1990. Extensive sodium. fire studies general survey of the ESMERALDA programme results. In: International Fast Reactor Safety Meeting, Snowbird, Utah, 12–16 Aug. 1990.
Mathé, E., 2014, Comportement des radiocontaminants dans les confinements d'un réacteur à neutrons rapides refroidi au sodium en situation accidentelle (Ph.D. thesis), Université Lille 1 Sciences et Technologie.
McCormack, J.D., Hilliard, R.K., Postma, A.K., 1978. Recent aerosol tests in the containment systems test facility. HELD-SA-1686.
Murata, K.K., Carroll, D.E., Bergeron, K.D., Valdez, G.D., 1993. CONTAIN LMR/1B-Mod. 1, A Computer Code for Containment Analysis of Accidents in Liquid-Metal-Cooled Nuclear Reactors, SAND-91-1490.
Souto, F.J., Haskin, F.E., Kmetyk, L.N., 1994. MELCOR 1.8.2 assessment: Aerosol experiments ABCOVE AB5, AB6, AB7 and LACE LA2. Sandia National Laboratories, SAND94-2166.
Subramanian, V., Baskaran, R., 2007. Initial size distribution of sodium combustion aerosol. Nucl. Technol. 160, 308–313.
Subramanian, V., Sahoo, P., Malathi, N., Ananthanarayanan, R., Baskaran, R., Saha, B., 2009. Studies on chemical speciation of sodium aerosols produced in sodium fire. Nucl. Technol. 165, 257–269.
Yamaguchi, A., Tajima, Y., 2006. A numerical study of radiation heat transfer in sodium pool combustion and response surface modeling of luminour flame emissivity. Nucl. Eng. Des. 236, 1179–1191.
Yamaguchi, A., Tajima, Y., 2009. Sodium pool combustion phenomena under natural convection airflow. Nucl. Eng. and Des. 239, 1331–1337.